DE GRUYTER Green Process Synth 2019; 8: 895–900

Santhanam Mohan and Manickam Vishnu Devan*

Photocatalytic activity of Ag/Ni bi-metallic nanoparticles on textile dye removal

https://doi.org/10.1515/gps-2019-0060
Received November 19, 2018; accepted July 14, 2019.

Abstract: The photocatalysis of Ag/Ni bi-metallic nanoparticles on safranin O dye degradation was evaluated by UV light irradiations. Ag/Ni bi-metallic nanoparticles were synthesized by the green approach using *Zingiber officinale* root (Zinger) extract. The average particles size of Ag/Ni bi-metallic nanoparticles was found to be 70-88 nm from SEM image and from XRD patterns it was confirmed that the existence of Ag/Ni bi-metallic nanoparticles. 8 mg of Ag/Ni bi-metallic nanoparticles present in 40 mL of 10 ppm dye, degraded completely in presence of UV light irradiations within 30 min time durations. The effect of dye degradation within a short period of time (30 min) was due to wide band gap energy and photochemical redox reactions.

Keywords: Z. root extract; Ag/Ni NPs; textile dye; SEM; UV and redox

1 Introduction

In the present scenario, the degradation of organic pollutants in water bodies is very important worldwide. Because of the untreated discharge of organic pollutants such as dyes, cosmetics, organic solvents etc. into the environment which causes short-term and long-term problems and most of the organic pollutants are carcinogen. Several wastewater treatments methods are available nowadays such as activated carbon, biodegradation, oxidation, the reduction that are costlier and more time-consuming. The photocatalytic dye degradation has several advantages that they are very effective in the degradation of dye in presence of sunlight irradiations.

Nobel metal nanoparticles have provided much application in bio-medical industries [1] besides photocatalysis. Bi-metallic nanoparticles synthesized by reduction of two metal combined by inter-metallic interactions in over nucleation process [2,3]. Ongoing exploited the noble Bi-metal nanoparticles such as (silver-gold, palladium-platinum, and silver-palladium and silver-nickel) have been applied in various areas like catalysis and medical ailments [4]. Especially Ag/Ni bi-metallic nanoparticles offering wide potential applications in bio-medical industries [5] and over the past decades a lot of chemical methods available for the preparation of Ag/Ni bi-metallic nanoparticles [6,7]. These route for more expensive, toxic, and potentially harmful to the eco-systems [8] but green strategy diverse for the synthesis of metal nanoparticles entities have significant role due to its environment friend viability and implies a simple, low-cost, with owing to their bio-medical and also catalytic applications [9]. Furthermore, the noble bi-metallic nanoparticles have superior photocatalytic activity towards the long-term disposal for dye removal. Phyto-fabrication of Ag/Ni bi-metallic nanoparticles is less toxic, highly reactive and low cost compared to other bi-metallic nanoparticles [10,11].

Here in this study, we have been synthesized Ag/Ni bi-metallic nanoparticles through the pyto-fabrication process for textile dye removal.

2 Experimental

2.1 Collections of plant materials and chemicals for the synthesis of Ag/Ni bi-metallic nanoparticles

The *Zingiber officinale* root was collected from the local farmhouse, Karur, Tamilnadu, India. Metal salts; silver nitrate, nickel nitrate were purchased from Merck, India and the textile dye ‘safranin O’ was purchased commercially. All the chemicals and reagents were used in the AR grade without any further purification. The whole experiment process was used in de-ionized water.

*** Corresponding author: Manickam Vishnu Devan,** Assistant Professor, PG and Research Department of Chemistry, Government Arts College, Karur-639005, Tamil Nadu, India
e-mail: devan70@ rediffmail.com
Santhanam Mohan, Department of Chemistry, Government Arts College, Karur-639005, Tamil Nadu, India

2.2 Preparation of capping agent

The *Zingiber officinale* root's (Z. root) visible particles were eradicated through running tap water in several times. The air-dried biomass was grounded to the powder with high-speed stainless steel blender. The 5% extract solutions were made in presence of 5 g of Z. root powder mixed with 100 mL of de-ionized water and then refluxed at 70°C for about 1 h. Later the homogeneous solutions were obtained and stored at 4°C. The prepared Z. root extract was used as a capping agent as well as the reducing agent for the synthesis of Ag/Ni bi-metallic nanoparticles (NPs) (Figure 1).

2.3 Synthesis of Ag/Ni bi-metallic nanoparticles

Monometallic (Ag, Ni) and bi-metallic (Ag/Ni) NPs were successfully modified by green reduction method using Z. root extract. A well-mixed binary aqueous solution was prepared using 60 mL of 1 mM $AgNO_3$ and 1 mM $Ni(NO_3)_2$ aqueous solution (1:1 ratio) and 10 mL of Z. root extracts was then added to this solution with the help of orbital shaker for about 1 h. in ambient temperature. The rapid reduction results in the formation of bi-metallic nanoparticles compared with the monometallic nanoparticles were synthesized in a similar manner. Here the formation of bi-metallic nanoparticles was used as a photocatalyst for dye degradation.

2.4 Photocatalytic inspections of silver/nickel bi-metallic NPs

Silver modified Ag/Ni bi-metallic nanoparticles were inspected for a photocatalytic activity of textile dye removal in the aqueous medium. Photo reactor was used as an artificial light source for UV light irradiation (mercury lamp-120 W). The aliquots 8 mg of the Ag/Ni NPs was added with 40 mL of (10 ppm/L) safranin O dye solution. The blank solution also set that was monitored with and without (Ag/Ni nanophotocatalyst). Later with the different time interval, the reaction mixture was subsequently measured by UV-visible spectrophotometer (model-Jasco-v-630). The rate of safranin O dye degradation was monitored in terms of the gradual decrease in the maximum absorbance peak at 518 nm:

Figure 1: *Zingiber officinale* root powder (synthesised from Zinger root).

$$\text{(\%) of degradation efficiency} = A_0 - A_R / A_0 \qquad (1)$$

where A_0 – blank solutions (without NPs), A_R – reaction mixture (with NPs).

3 Results and discussion

3.1 Surface plasmon resonance study (SPR) to confirm the formation Ag/Ni bi-metallic NPs

The surface plasmon resonance study by UV-Visible spectroscopic study was conducted to confirm the formation of silver mono and silver/nickel bi-metallic nanoparticles as shown in Figure 2. The formation of silver mono and silver/nickel bi-metallic nanoparticles were due to the reduction of mono and bi-metallic (Ag^+, Ni^{2+} and Ag0 and Ni0 NPs) by bio-active molecules present in the Z. root extract. The broad peaks at 420 nm and 461 nm confirmed the reduction of Ag^+ and Ag^+/Ni^{2+} to zero valent Ag and Ag/Ni NPs by Z. root extract. The colour transformation from yellowish to deep brown color indicates the formation of mono and bi-metallic nanoparticles [12]. The energy gap was calculated using Eq. 2:

$$E_g = \frac{1240}{\lambda} \text{ eV} \qquad (2)$$

where: λ – maximum absorbance, E_g – energy gap (eV). The energy gap value of Ag/Ni bi-metallic nanoparticles was found to be 2.6 eV.

3.2 Functional group analysis of silver/nickel bi-metallic nanoparticles by FT IR

Functional groups present in Ag/Ni NPs were characterized by FT IR spectrum which was shown in Figure 3. FT IR spectrum of Ag/Ni NP observed that strong and broad peaks at 3420.2 cm^{-1} and 1634.7 cm^{-1} which confirmed the binding of υ(-OH) and υ (–NH_2) poly-phenols along with amino acids with Z. root extract. Another peak was assigned at 1356.3 cm^{-1} was due to υ(C=C) aromatic stretching [13]. The presence of polyphenols and amino acids in the pyto components confirmed by FT IR spectrum were responsible for the reduction of silver and nickel ions into silver/nickel bi-metallic nanoparticles respectfully.

3.3 Structural and morphological characterization of Ag/Ni bi-metallic nanoparticles

The morphology of green synthesized Ag/Ni bi-metallic NPs was performed by SEM. Figures 4a and 4b show well-poly dispersed Ag/Ni bi-metallic NPs has identified in the sizes range of 70-88 nm. The particles were clearly identified by their spherical-like shapes with no agglomeration [14,15]. Figure 4d represents the elemental composition of Ag/Ni bi-metallic nanoparticles which was examined by EDX spectroscopic techniques. The successful formation of Ag/Ni bi-metallic nanoparticles was shown in Figure 4b attributed the strong peaks in the Ag, Ni was confirmed at 3 eV [16].

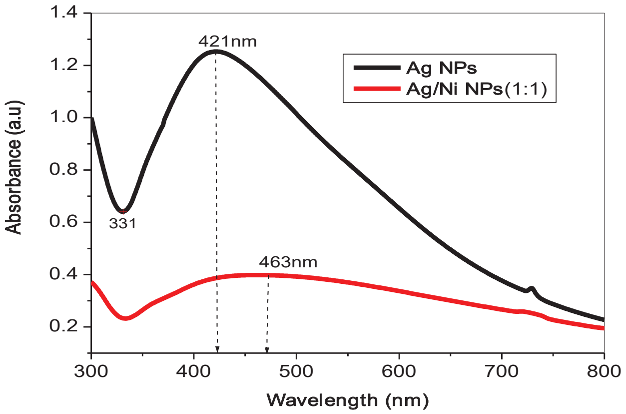

Figure 2: UV-Visible absorption spectra of mono and bi-metallic nanoparticles using Z. root extract.

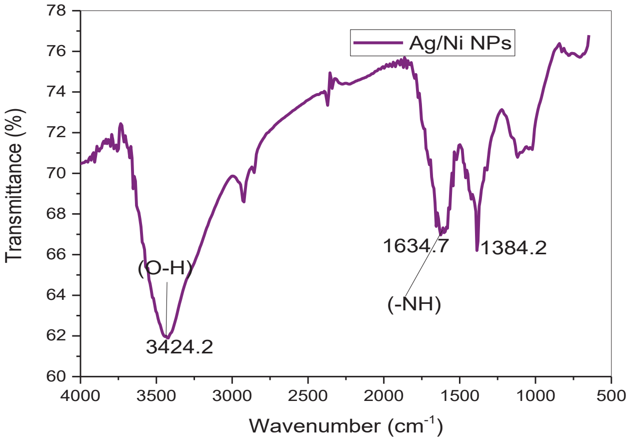

Figure 3: FT IR spectrum of silver/nickel bi-metallic nanoparticles using Z. root extract.

Figure 4c shows that Ag, Ni mono and Ag/Ni bi-metallic catalyst was in crystallite nature by powder X-ray diffraction patterns. The three diffraction peaks allocated at 39.4°, 45.6°, 58.2° and 65.7° the appropriate the lattice planes (111)*, (200), (220) and (311) were corresponding to the silver, nickel mono and silver/nickel bi-metallic nanoparticles respectively. The prominent peaks (111)* should be agree compared with the silver, nickel nanoparticles respectively [16]. The Ag/Ni bi-MNPs average crystallite size was calculated using this equation of Debye-Scherrer formula:

$$D = k\lambda / \beta \, \text{Cos}\theta \tag{3}$$

where: D is the average crystalline size of the nanoparticles, k is geometric factor (0.9), λ is the wavelength of X-ray diffraction source and β is the angular FWHM (full width at half maximum) of the XRD peak at the diffractions angle θ.

3.4 Fluorescent studies of silver, nickel mono, and silver/nickel bi-metallic nanoparticles

Fluorescence spectroscopy studies was carried out to examine the fluorescence property of mono and bi-metallic metallic nanoparticles. The excited peak at 502 nm and green-red emission of fluorescent was observed at 854 nm for Ag/Ni bi-metallic nanoparticles which were shown in Figure 5. This may be due to inter-metallic interactions of fluorescent emission and bi-metallic nanoparticles surface area, may shift the electron band of silver, nickel mono to silver/nickel bi-metallic nanoparticles and the excitation of Fermi level sp (or) d band holes [17].

3.5 Kinetic parameters

A kinetic plot of the SO dye degradation with respect to the irradiation time and fit linear relationship (Figure 6b) and thus exhibits pseudo-first order kinetics:

$$\ln(C_0 / C_t) = K_{app}t \tag{4}$$

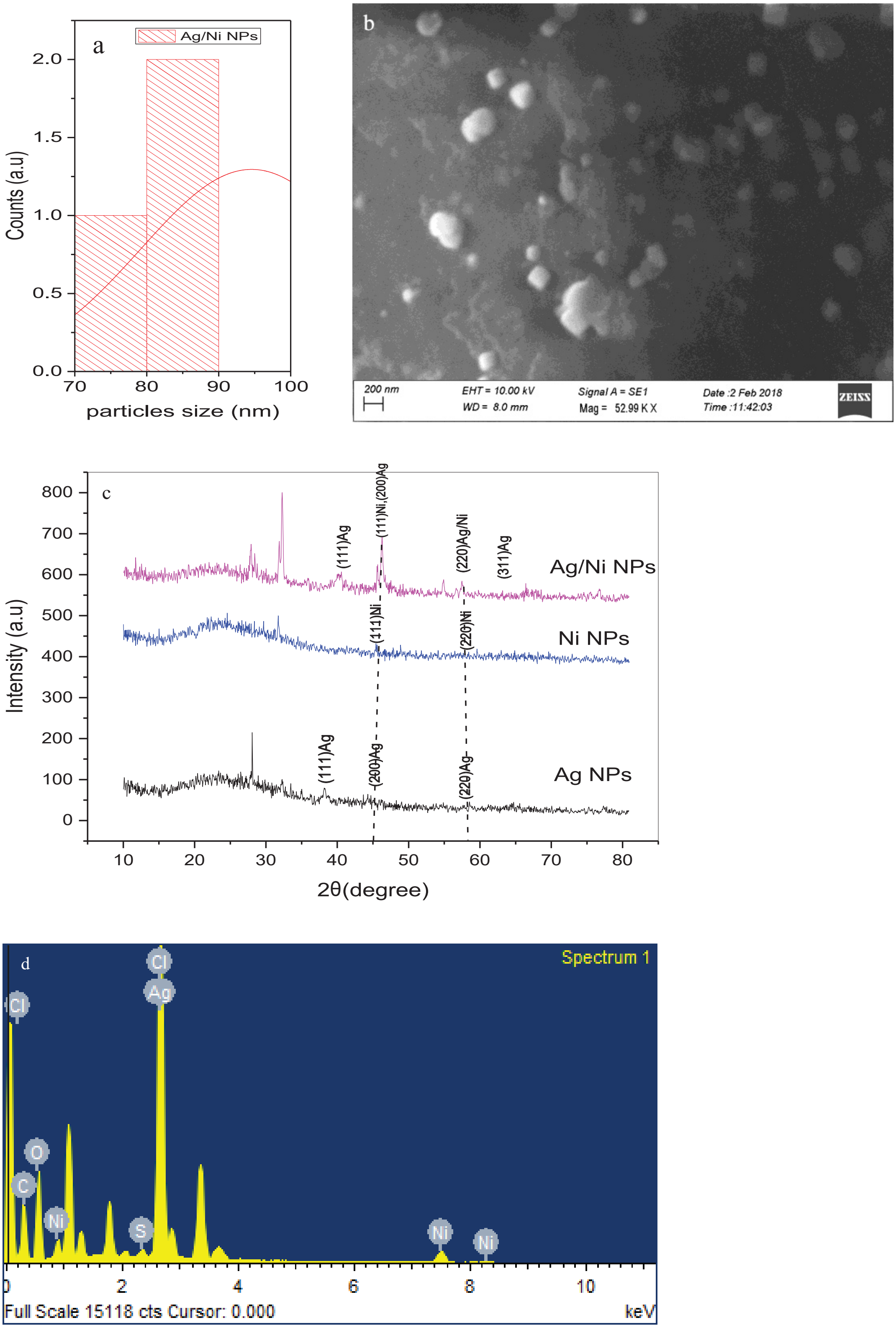

Figure 4: (a,b) Morphological study of Ag/Ni bi-metallic NPs by SEM and its particle size distribution; (c) XRD pattern of Ag/Ni bi-metallic NPs; (d) EDX spectrum of Ag/Ni bi-metallic NPs.

where: $k_{app}t$ (min^{-1}) is the apparent rate constant and pseudo rate constant (k) was found to be 0.00859 min^{-1}. C_o is the initial concentration of the dye and C is the concentration at time t. Furthermore, the regression of coefficient (R^2) of 0.98 confirmed that the photo degradation of SO dye fitted the Langmuir–Hinshelwood kinetic model [18].

3.6 Mechanisms of photocatalysis

The light-induced mechanisms proposed by photocatalysis method using safranin O textile dye removal were shown in Figure 6a. The photocatalysis of safranin O textile dye removal was played a crucial role in UV light irradiations. When an event UV light strikes on the silver/nickel bi-metallic nanoparticles surface layer, the excitation of the valence electron of silver/nickel bi-metallic nanoparticles occurs with the formation of electron-hole pairs. These electron-hole pairs create reactive oxygen species (ROS). Finally, the hydroxyl free radicals and superoxide ions were responsible for the removal of textile dye in aqueous phase.

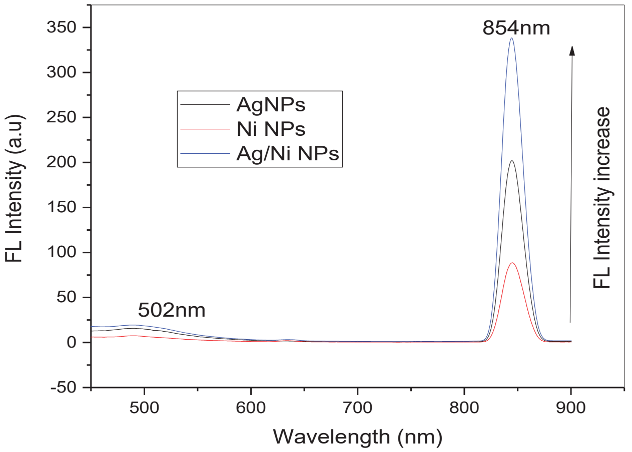

Figure 5: Fluorescence spectrum of silver, nickel mono and silver/nickel bi-metallic nanoparticles using Z. root powder extract.

3.7 Quantum yield of Ag/Ni NPs on saffranin O dye degradation

Quantum yield of silver/nickel bi-metallic nanoparticles on safranin O dye degradation was calculated using this formula:

$$\Phi = \text{No of molecules decomposed / No of photons absorbed} \quad (5)$$

The observed Quantum yield of silver/nickel bi-metallic nanoparticles for this study is found to be (Φ) = 2.37 which indicates if the Quantum Yield is >1 then by absorbing per Quantum of a photon, a large number of reactant molecules (dye) undergo decomposition.

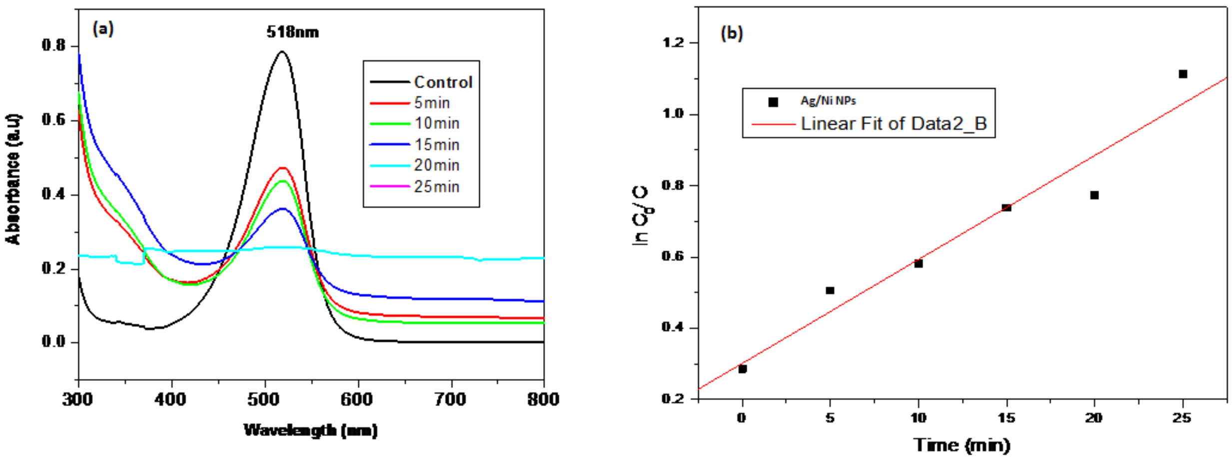

Figure 6: (a) UV-Visible absorption spectrum of safranin O textile dye degradation in absence and presence of silver/nickel bi-metallic nanoparticles using photocatalysis method; (b) Kinetic plot of safranin O textile dye degradation.

4 Conclusion

Silver modified silver/nickel bi-metallic nanoparticles was successfully synthesized by a low-cost and conventional green route using *Zingiber officinale* root. The optical and structural properties were characterized by UV-Visible, FTIR, and a surface morphological study was confirmed by SEM-EDX spectroscopic studies reveals that the synthesized nanoparticles were in nanoscale. The silver/nickel bi-metallic nanoparticles have completely degraded safranin O textile dye in presence of UV light irradiation within 30 min time durations. The effect of dye degradation within a short period of time was due to a large band gap 2.6 eV and photochemical redox reactions. Further, the red emission from the luminescent study confirmed the photo catalytic dye degradation on safranin O textile dye. From this above observation, it is concluded that besides degradation of textile dye, the Ag/Ni bi-metallic NPs may also be used in optoelectronics devices, bio-imaging and in nanomedicine.

Acknowledgements: This research did not receive any specific grant from funding in the public or from commercial sectors.

References

[1] Mallikarjuna N.N., Verma R.S., Green synthesis of silver and palladium nanoparticles at room temperature using coffee and tea extract. Green Chem., 2008, 10, 859-862.

[2] Sperling R.A., Rivera G., Zanella M., Parak W.J., Biological Application of Gold Nanoparticles. Chem. Soc. Rev., 2008, 37, 1896-1908.

[3] Nadagouda M.N., Varma R.S., Synthesis of thermally stable carboxymethyl cellulose/metal biodegradable nanocomposites for potential biological applications. Biomacromolecules, 2007, 8, 2762-2767.

[4] Dahl J.A., Maddux L.S., Hutchison J.E., Toward Greener Nanosynthesis. Chem. Rev., 2007, 107, 2228-2269.

[5] Loo C., Lowery A., Halas N., West J., Drezek R., Immunotargeted Nanoshells for Integrated Cancer Imaging and Therapy. Nano Lett., 2005, 5, 4, 709-711.

[6] Lee C.-C., Chen D.-H., Large-scale synthesis of Ni-Ag core-shell nanoparticles with magnetic, optical and anti-oxidation properties. Nanotechnology, 2006, 17, 3094.

[7] Ouyang R., Zhang W., Zhou S., Yang Y., Ji Y., Feng K., et al., Single Walled Carbon Nanotube Sandwiched Ni-Ag Hybrid Nanoparticle Layers for the Extraordinary Electrocatalysis toward Glucose Oxidation. Electrochimic. Acta, 2016, 188, 197-209.

[8] Ubonchonlakate K., Sikong L., Tontai T., Saito F., *P. aeruginosa* Inactivation with Silver and Nickel Doped TiO2 Film Coat on Glass Fiber Riving Adv. Mater. Res., 2010,150-151, 1726-1731.

[9] Leopold N., Lendl B., A New Method for Fast Preparation of Highly Surface-Enhanced Raman Scattering (SERS) Active Silver Colloids at Room Temperature by Reduction of Silver Nitrate with Hydroxylamine Hydrochloride. J. Phys. Chem. B, 2003, 107, 5723-5727.

[10] Nasrollahzadeh M., Atarod M., Jaleh B., Gandomirouzbahani M., Biosynthesis of Silver Nanoparticles using Almond Plantleaf extract and their Antibacterial Activity. Ceram. Int., 2016, 42, 8587-8596.

[11] Muthu K., Priya S., Green synthesis, characterization and catalytic activity of silver nanoparticles using *Cassia auriculata* flower extract separated fraction. Spectrochimi. Acta A, 2017, 179, 66-72.

[12] Akinsiku A.A., Dare E.O., Ajanaku K.O., Ajani O.O., Olugbuyiro J.A.O., Siyanbola T.O., et al., Modeling and Synthesis of Ag and Ag/Ni Allied Bimetallic Nanoparticles by Green Method: Optical and Biological Properties. Int. J. Biomater., 2018, 9658080,1-17, DOI:10.1155/2018/9658080.

[13] Kolya H., Maiti P., Pandey A., Tripathy T., Green synthesis of silver nanoparticles with antimicrobial and azo dye (Congo red) degradation properties using *Amaranthus gangeticus* Linn leaf extract. J. Anal. Sci. Tech., 2015, 6(33), DOI:10.1186/s40543-015-0074.

[14] Basu S., Maji P., Ganguly J., Rapid green synthesis of silver nanoparticles by aqueous extract of seeds of *Nyctanthes arbor-ristis*. J. Appl. Nanosci., 2016, 6(1), 1-5.

[15] Mntungwa N., Pullabhotla V.S.R., Revaprasadu N., Facile Synthesis of Organically Capped CdTe Nanoparticles. J. Nanosci. Nanotechno., 2012, 12(3), 2640-2644.

[16] Adekoya J.A., Dare E.O., Mesubi M.A., Revaprasadu N., Synthesis and Characterization of Optically Active Fractal Seed Mediated Silver Nickel Bimetallic Nanoparticles. J. Mater., 2014, 1-9, DOI:10.1155/2014/184216.

[17] Angshuman P., Sunil S., Surekha D., Microwave-assisted synthesis of silver nanoparticles using ethanol as a reducing agent. Mater. Chem. Phys., 2009, 114, 530-532.

[18] Khezrianjoo S., Revanasiddappa H.D., Langmuir-Hinshelwood Kinetic Expression for the Photocatalytic Degradation of Metanil Yellow Aqueous Solutions by ZnO Catalyst. Chem. Sci. J., 2012, CSJ-85.